Spectrum Sharing Backhaul Satellite-Terrestrial Systems via Analog Beamforming

Miguel Ángel Vázquez, Luis Blanco and Ana I. Pérez-Neira, *Senior Member, IEEE*

***Abstract*—Current satellite and terrestrial backhaul systems are deployed in disjoint frequency bands. This fact precludes an efficient use of the spectrum and limits the evolution of wireless backhauling networks. In this paper, we propose an interference mitigation technique in order to allow the spectrum coexistence between satellite and terrestrial backhaul links. This interference reliever is implemented at the terrestrial backhaul nodes which are assumed to be equipped with multiple antennas. Due to the large bandwidth and huge number of antennas required in these systems, we consider pure analog beamforming. Precisely, we assume a phased array beamforming configuration so that the terrestrial backhaul node can only reduce the interference by changing the phases of each beamforming weight. Two cases are considered: the 18 and 28 GHz band where transmit and receive beamforming optimization problems shall be tackled respectively. In both cases, the optimization problem results in a non-convex problem which we propose to solve via two alternative convex approximation methods. These two approaches are evaluated and they present less than 1 dB array gain loss with respect to the upper bound solution. Finally, the spectral efficiency gains of the proposed spectrum sharing scenarios are validated in numerical simulations.**

***Keywords*—Beamforming, satellite communications, backhaul systems, non-convex QCQP, phase-only beamforming.**

I. Introduction

Future exponential user data rate demands will not only impact the radio access technology but also the backhauling mechanisms. Indeed, these backhaul services are meant to be ubiquitous, offering extremely high rate wireless connectivity in order to reduce the capital expenditures. With the aim of attending to these demands, the spectral efficiency of the frequency bands where these services are currently deployed shall be increased.

In here, we consider the millimeter wave (mmWave) bands of $17.3 - 20.2$ GHz and $27.5 - 30$ GHz currently utilized by fixed satellite services (FSS) and backhaul fixed services (FS). These two portions of the spectrum are currently fragmented by FSS exclusive use, FS exclusive use and shared for both services [1]. Despite the spectrum regulation permits spectrum sharing, neither FS nor FSS deploy their services in shared bands as no interference protection can be claimed.

According to the recent results in cellular mmWave spectrum sharing techniques, due to the high directional antennas used, very large spectral efficiencies can be obtained if multiple transmitters share the spectrum [2]–[5]. In addition, the authors in [6], [7] consider the spectrum sharing between FSS and mmWave cellular systems and they propose different configurations for keeping the interference towards the FSS terminals low.

The shared use of the spectrum between FS and FSS is also studied in [8], [9]. The authors in [8] propose the use of databases jointly with spectrum sensing for dynamically allocate the spectrum for FS and FSS. In addition, the use multiple low noise blocks (LNB) at the FSS is analyzed in both [8] and [9] for mitigating the interference with the aim of using a more aggressive frequency reuse among FS and FSS.

Interference between FS and FSS has been identified in [10], precluding an efficient use of the spectrum in certain cases. This paper focuses on interference mitigation techniques for supporting the spectrum sharing between FS and FSS. In particular, we consider that the FS terminals are equipped with multiple antennas with the objective of not only obtaining a high gain towards the intended link, but also to reduce the interference towards the non-intended receivers. Alternatively, we consider that the FSS terminals are only equipped with a single antenna.

Our approach differs to the previous commented works: the use of multiple antennas in the FS links has not been addressed before for interference mitigation. Two main cases are considered. In the $17.3 - 20.2$ GHz band devoted to the satellite forward link (space to Earth communication), we design the FS transmit beamforming that shall keep the interference towards the FSS terminals under a certain threshold. In addition, we consider the $27.5 - 30$ GHz band dedicated to the satellite return link (Earth to space transmission) where the FS terminals shall design their receive beamforming in order to mitigate the received FSS interference.

Since fully-digital transceivers cannot be used due to its tremendous cost and complexity [11], we resort to analog beamforming schemes. In particular, we focus on phased array architectures where the transceiver is only equipped with a single radio frequency chain and the spatial processing is done through phase shifters. Note that in backhauling mmWave transmissions, the scattering is expected to be limited and; thus, the resulting channel matrix generally only admits a single-stream transmission (i.e. beamforming) [12].

This work has received funding from the European Union's Horizon 2020 research and innovation programme under grant agreement No 645047 (SANSA); the Spanish Ministry of Economy and Competitiveness (Ministerio de Economia y Competitividad) under project TEC2017-90093-C3-1-R (TERESA); and from the Catalan Government (2017-SGR-1479, 2017-SGR-891).

M. Á. Vázquez and Luis Blanco are with Centre Tecnològic de les Telecomunicacions de Catalunya (CTTC), Barcelona, Spain. Ana I. Pérez-Neira is with Universitat Politecnica de Catalunya (UPC) and CTTC.

Emails: mavazquez@cttc.es, lblanco@cttc.es, ana.perez@cttc.es

Phased arrays present less flexibility than digital beamforming solutions. While fully-digital schemes can vary not only the phase and amplitude of the beamforming weights, phased arrays can only change their phase, keeping its magnitude fixed. In this context, the traditional beamforming designs for spectrum sharing systems [13], [14] must be revisited to become phase-only designs.

Despite the recent works on phase-only beamforming [15]–[17], little is known about interference mitigation techniques using this multiantenna configuration. To the best of authors knowledge, the work in [18] is the first one considering interference mitigation via phase-only beamforming.

We first introduce the fully-digital optimization problems and; posteriorly, we describe and remark the differences with the phased array (phase-only) problems. Both transmit and receive phase-only beamforming designs lead to non-convex quadratically constraint quadratic programs (QCQP) due to the equality quadratic constraints imposed by the phase-only restrictions. These problems are difficult to solve and convex relaxation techniques are required. We resort to two different alternatives based on the concave-convex procedure (CCP) [19]. First, we consider the equivalent semidefinite program (SDP) reformulation and we apply the CCP method on the rank one constraint. Alternatively, we consider the penalized CCP (PCCP) presented in [20] of the original QCQP scheme. Both approaches behave better than the SDP relaxation (SDR) and Gaussian randomization method [21] which is known to be inefficient when there are dual-side constraints [22], [23].

To sum up, the contributions of the paper are the following:

1) We propose two optimization frameworks for dealing phase-only beamforming optimization, namely SDP-CCP and QCQP-PCCP. While the transmit case SDP-CCP is preliminary studied in [18], QCQP-PCCP is a new scheme specially adapted for this problem. In addition, the design of phase-only receive beamforming is novel.
2) The proposed optimization frameworks are compared in terms of performance and computational complexity. Interestingly, the most adequate optimization framework varies whether we consider the receive or transmit beamforming problem.
3) The achievable rates of the shared use of the spectrum between FS and FSS are evaluated in the $17.3-20.2$ GHz and $27.5-30$ GHz bands. We observe a significant spectral efficiency gain by using the proposed interference mitigation techniques.

The paper is organized as follows. Section II describes the system and channel model. Section III presents the receive and transmit analog beamforming optimization problems. Section IV proposes two optimization frameworks for optimizing the described problems. Section V depicts the numerical simulation results and Section VI concludes.

Notation: Throughout this paper, the following notations are adopted. Boldface upper-case letters denote matrices and boldface lower-case letters refer to column vectors. $(.)^H$, $(.)^T$, $(.)^*$ denote a Hermitian transpose, transpose, and conjugate matrix, respectively. $||.||$ refer to the expected value operator and the Frobenius norm, respectively. $[\mathbf{x}]_i$ denotes the i-th element of vector $\mathbf{x}$. $|\cdot|$ denotes the absolute value operator. $\circ$ denotes the Hadamard matrix product. $\mathrm{Tr}\,(\cdot)$ denotes the trace operator. $\mathbf{A} \succ 0$ describes the set of semidefinite positive matrices $\mathbf{A}$. The vector $\mathbf{z}^{H,(n)}$ is the conjugate transpose of vector $\mathbf{z}^{(n)}$.

II. System Model and channel model

Let us consider a FS link (i.e. a fixed wireless link between terrestrial entities) where the transmitter is equipped with N_T antennas and the receiver with N_R antennas in the shared 18 GHz band. In this portion of the spectrum, satellite receivers can be deployed but they cannot claim protection from the FS links. The received signal at the FS receiver can be modelled by

$$\mathbf{y}_{FS} = \mathbf{H}\mathbf{v}s + \mathbf{n}, \tag{1}$$

where $\mathbf{H} \in \mathbb{C}^{N_R \times N_T}$ is the channel matrix, $\mathbf{v} \in \mathbb{C}^{N_T \times 1}$ is the transmit beamforming, s is the transmitted symbol with zero mean and unit energy and $\mathbf{n}$ is the additive white Gaussian noise term with zero mean and covariance matrix $\frac{\sigma_{FS}^2}{N_R}\mathbf{I}$.

In the 18 GHz band, the FS transmission takes place in presence of K very small aperture terminal (VSAT) satellite receivers. These VSATs are terminals that enable the FSS. That is, VSATs receive data from the satellite forward link (from space to Earth). The received signal of the k-th VSAT can be modelled by

$$y_{\text{VSAT},k} = \mathbf{g}_k^H \mathbf{v}s + w_k, \tag{2}$$

where $\mathbf{g}_k \in \mathbb{C}^{N_T \times 1}$ is the channel vector between the FS transmitter and the k-th VSAT receiver and w_k is the noise term of the k-th VSAT receiver assumed to be Gaussian zero mean with variance σ_{VSAT}^2.

The considered backhauling systems could be deployed in the 28 GHz band which is used by VSATs for the return link transmission (from Earth to space). These transmission would interfere the FS links deployed at the 28 GHz. Mathematically, the received signal of a FS link in presence of M interfering VSATs is

$$z_{FS} = \mathbf{u}^H \left(\mathbf{H}\mathbf{t}s + \sum_{m=1}^{M} P_{\text{VSAT},m}\mathbf{p}_m s_{VSAT,m} + \mathbf{n} \right) \tag{3}$$

where $\mathbf{u} \in \mathbb{C}^{N_R \times 1}$ is the receive beamforming, $\mathbf{t} \in \mathbb{C}^{N_T \times 1}$ is the transmit beamforming, $\mathbf{p}_m \in \mathbb{C}^{N_R \times 1}$ is the channel vector between the m-th VSAT transmitter and the FS receiver, $s_{\text{VSAT},m}$ is the zero mean unit energy symbol transmitted by the m-th VSAT, $P_{VSAT,m}$ its transmit power and $\mathbf{n}$ the noise term assumed to be Gaussian with zero mean and variance equal to σ_{VSAT}^2. Figure 1 describes both system models. As a matter of fact, the mmWave backhaul channel modelling has not been deeply addressed. Indeed, the literature has been focused on mmWave urban and cellular systems [24]. To the best of author's knowledge, the work in [25, Section 5.7] is the only one reporting the channel modelling parameters for backhauling scenarios. In this context, the channel modelling can be described as follows

$$\mathbf{H} = \gamma \frac{1}{\sqrt{L}} \sum_{c=1}^{C} \sum_{l=1}^{L} \alpha_{cl} \mathbf{a}_{rx}\left(\theta_{cl}^{rx}, \phi_{cl}^{rx}\right) \mathbf{a}_{tx}\left(\theta_{cl}^{tx}, \phi_{cl}^{tx}\right)^H, \tag{4}$$

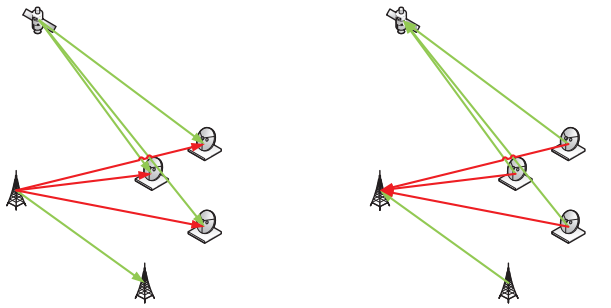

Fig. 1. Schematic of the considered scenarios where the red lines represent the interference signals and the green ones the legitimate transmissions. On the left it is depicted the 18 GHz band case where the FS interfere with the VSATs. Figure on the right describes the 28 GHz shared band case where the VSATs interfere the FS links.

where L denote the number of sub-paths and C the number of clusters. The value α_{cl} is a small scale fading term of the l-th sub-path at the c-th cluster for $c > 1$ and $l > 1$ otherwise, for the value α_{11} is assumed to be equal to one. Vectors $\mathbf{a}_{tx}(\cdot,\cdot) \in \mathbb{C}^{N_T \times 1}$ and $\mathbf{a}_{rx}(\cdot,\cdot) \in \mathbb{C}^{N_R \times 1}$ are the antenna responses of both the transmitter and the receiver respectively. The transmit and receive antenna responses depend on both the angles of departure (AoD), $\theta_{cl}^{tx}, \phi_{cl}^{tx}$, and angles of arrival (AoA), $\theta_{cl}^{rx}, \phi_{cl}^{rx}$, respectively.

The small scale fading can be modelled as

$$\alpha_{cl} = A_{cl} e^{\psi_{cl} j}, \tag{5}$$

where A_{cl} is Rayleigh distributed with mean 0.1 and ψ_{cl} is uniformly distributed from 0 to 2π. We assume that $\theta_{11}^{tx}, \theta_{11}^{rx}, \phi_{11}^{tx}, \phi_{11}^{rx}$ are deterministic and it can be computed by known the relative positions between the transmitter and the receiver. In addition, for $c > 1$ and $l > 1$, we assume that

$$\theta_{cl}^{tx} = \theta_{11}^{tx} + \chi^{tx}, \phi_{cl}^{tx} = \phi_{11}^{tx} + \psi^{tx} \tag{6}$$

$$\theta_{cl}^{rx} = \theta_{11}^{rx} + \chi^{rx}, \phi_{cl}^{rx} = \phi_{11}^{rx} + \psi^{rx}, \tag{7}$$

where χ^{tx}, ψ^{tx}, ψ^{rx} and χ^{rx} are zero mean Gaussian distributed random variables with standard deviation equal to 5.

The steering vectors $\mathbf{a}_{tx}(\cdot,\cdot)$ and $\mathbf{a}_{rx}(\cdot,\cdot)$ depend on the antenna array structure and the element spacing. For the FS terminals, we consider the uniform rectangular array (URA) whose steering vector can be written as

$$\mathbf{a}_{\text{URA}}(\theta,\phi) = \text{vec}\left(\mathbf{a}_x(\theta,\phi)\,\mathbf{a}_y(\theta,\phi)^T\right), \tag{8}$$

where $\mathbf{a}_x$ and $\mathbf{a}_y$ are (9) and (10) respectively. N_x, N_y are the number of elements in the horizontal and vertical dimension, d_x, d_y the element spacing in the horizontal and vertical dimension and λ the wavelength. For the sake of simplicity and without loss of generality we assume $N_x N_y = N_T = N_R$.

Note that we have not considered the non-line-of-sight (NLOS) component of channel modelling which have been described in several works [26]. This is because we focus on backhaul cellular networks which are generally deployed in isolated towers at rural areas or above the rooftop at urban scenarios [25]. For radio access architectures, NLOS channel impact is of key importance and it must be considered.

The antenna response of the VSATs can be written as

$$a_{VSAT}(\theta,\phi) = \sqrt{G_{\max} G(\theta,\phi)} \tag{11}$$

where $G_{\max}$ is the maximum antenna gain and $G(\theta,\phi)$ describes the antenna radiation pattern of the VSAT and it can be obtained from ITU-R S.465-6 [27]. Finally, γ for denotes the path-loss which can be written as

$$\gamma = \left(\frac{1}{4\pi d\lambda}\right), \tag{12}$$

where d is the distance between the transmitter and the receiver.

To sum up, this paper considers two spectrum sharing scenarios:

1) Scenario A: At 17.3-20.2 GHz where a satellite forward link transmission (i.e. space to Earth link) and FS links could coexist.
2) Scenario B: At 27.5-30.0 GHz where a satellite return link transmission (i.e. Earth to space link) and FS links could coexist.

In both cases, we consider that the FS terminals (transmit and receive) have multiple antennas and the FSS links have a single antenna. In this context, the role of the FS terminals is different at each scenario: while in scenario A, they have to restrict the created interference to the FSS; in scenario B they have to mitigate the interference that they receive from the FSS. This is, we do not consider that the FSS terminals perform interference mitigation. This approach will support the deployments in the mentioned spectrum sharing scenarios without updating the FSS terminals equipment.

It is important to remark that despite we consider transmit and receive beamforming for the FS links, this paper does not tackle the transmit and receive joint optimization problem. Instead, we consider transmit and receive beamforming optimization separately, addressing the 18 and 28 GHz bands sub-problems respectively.

III. Beamforming Optimization Problem Statements

This Section presents the optimization problems to be tackled in order to allow the spectrum sharing coexistence of FSS and FS links. Precisely, the beamforming optimization is presented both at the transmit and receive side of the FS links. We present both the fully-digital and fully-analog beamforming solutions, which offer a substantial different cost. Indeed, while the fully-digital solution requires either N_T or N_R RF chains at both the receiver and the transmit side, the fully-analog scheme only requires a single RF chain. Figures 2 and 3 depict the fully-digital and fully-analog beamforming solutions.

$$\mathbf{a}_x(\theta,\phi) = \frac{1}{\sqrt{N_x}}\left(1, e^{j\frac{2\pi}{\lambda}d_x\sin(\theta)\cos(\phi)}, \ldots, e^{j\frac{2\pi}{\lambda}(N_x-1)d_x\sin(\theta)\cos(\phi)}\right)^T \tag{9}$$

$$\mathbf{a}_y(\theta,\phi) = \frac{1}{\sqrt{N_y}}\left(1, e^{j\frac{2\pi}{\lambda}d_y\sin(\theta)\sin(\phi)}, \ldots, e^{j\frac{2\pi}{\lambda}(N_y-1)d_y\sin(\theta)\sin(\phi)}\right)^T \tag{10}$$

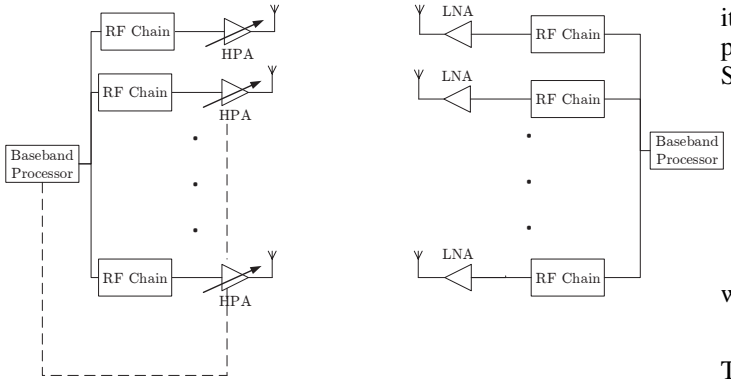

Fig. 2. Fully-digital FS beamforming. In contrast to an all-analog scheme, this architecture spatially processes the data in a baseband processor which offers a large flexibility in terms of operations.

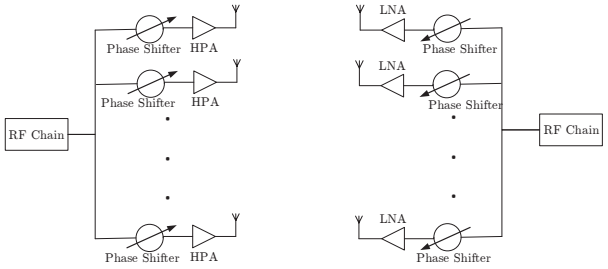

Fig. 3. Fully-analog FS beamforming. In contrast to an all-digital scheme, the spatial processing can only be done in analog domain through phase-shifters. Note that the power amplifiers are fixed to a transmit power that cannot be modified.

A. Transmit Beamforming Optimization Problem (Scenario A)

The transmit beamforming optimization with an all-digital architecture can be mathematically described as follows

$$\underset{\mathbf{v}}{\text{maximize}} \quad \|\mathbf{H}\mathbf{v}\|^2 \tag{13a}$$
$$\text{subject to} \tag{13b}$$
$$|\mathbf{g}_k^H\mathbf{v}|^2 \leq \epsilon_k \quad k=1,\ldots,K, \tag{13c}$$
$$\|\mathbf{v}\|^2 \leq P \tag{13d}$$

where P is the maximum available power and ϵ_k the maximum allowed array gain value towards the k-th VSAT. The optimization problem in (13) aims to maximize the data rate of the FS link while keeping an interference constraint towards the FSS receivers. By modifying ϵ_k we can control the interference power signal received by the FSS receiver.

The optimization problem (13) is a non-convex QCQP since it is the maximization of a convex function. The optimization problem in (13) can be relaxed to a convex problem with the SDR method. This technique relaxes the original problem into

$$\begin{aligned} &\underset{\mathbf{V}\succeq 0}{\text{maximize}} \quad \text{Tr}\left(\overline{\mathbf{H}}\mathbf{V}\right) \\ &\text{subject to} \\ &\text{Tr}\left(\mathbf{G}_k\mathbf{V}\right) \leq \epsilon_k \quad k=1,\ldots,K, \\ &\text{Tr}\left(\mathbf{V}\right) \leq P, \end{aligned} \tag{14}$$

where

$$\overline{\mathbf{H}} = \mathbf{H}\mathbf{H}^H, \mathbf{G}_k = \mathbf{g}_k\mathbf{g}_k^H. \tag{15}$$

The optimization problem in (14) is the SDR of the optimization problem in (13). That is, if we include in (14) an additional constraint

$$\text{rank}\left(\mathbf{V}\right) = 1, \tag{16}$$

where $\text{rank}\left(\cdot\right)$ denotes the rank operator; the optimization problems in (14) and (13) are equivalent.

The optimization problem (14) is a semidefinite program which is convex and; thus, it can be solved via interior point methods. Indeed, whenever the optimal solution of (14) denoted by $\mathbf{V}^\star$ is rank one, the SDR is tight and the optimal solution of the original problem (13) can be obtained by computing the eigenvector associated to the maximum eigenvalue of $\mathbf{V}^\star$. Nevertheless, the optimal solution $\mathbf{V}^\star$ is generally high rank so that Gaussian randomization methods are required. These methods are based on the creation of a large number of Gaussian randomization instances with zero mean and covariance matrix equal to $\mathbf{V}^\star$. Among all realizations, it is selected the one with the best performance (the best array gain for our case) that does not violate the constraints. The reader can refer to [21] for further details.

Whenever the transmitter can only modify the phases of the beamforming weights, the optimization problem in (13) becomes

$$\underset{\mathbf{v}}{\text{maximize}} \quad \|\mathbf{H}\mathbf{v}\|^2 \tag{17a}$$
$$\text{subject to} \tag{17b}$$
$$|\mathbf{g}_k^H\mathbf{v}|^2 \leq \epsilon_k \quad k=1,\ldots,K, \tag{17c}$$
$$|[\mathbf{v}]_n|^2 = P/N_T \quad n=1,\ldots,N_T \tag{17d}$$

where the main difference compared to (13) is (17d), which are the phase-only beamforming constraints. Even though a priori these new set of constraints do not impact on the optimization problem, it entails a major difficulty for the SDR and; specifically, for the Gaussian randomization. This is described in the following.

Considering the SDR relaxation in (14) with the corresponding phase-only set of constraints (17d) and $\mathbf{V}^\star$ not being rank

one, the Gaussian randomization technique computes a vector Gaussian random variable with zero mean and covariance matrix $\mathbf{V}^{\star}$. With this variable, $\mathbf{v}^{\text{rand}}$, the system designer has to obtain a feasible solution of (17). This feasible solution is imposed by the phase-only restrictions which require that the randomization is transformed into

$$\mathbf{v}_k^{\text{rand}} \leftarrow \mathbf{v}^{\text{rand}} \circ \mathbf{f}, \tag{18}$$

where

$$\mathbf{f} = \left(\frac{1}{|[\mathbf{v}^{\text{rand}}]_1|}, \ldots, \frac{1}{|[\mathbf{v}^{\text{rand}}]_{N_T}|} \right)^T. \tag{19}$$

In other words, the scaling factor is not unique. This fact differs from other optimizations that have used SDR. This is the case of the multigroup multicast optimization [28], [29] where after the Gaussian randomization the SDR requires a scaling factor optimization bearing in mind the constraints. This technique cannot be applied here as there is no flexibility in the scaling factor. As a result, the SDR leading to a high rank solution has an enormous difficulty of delivering a feasible rank one solution due to the equality constraints. Numerically, we observed the performance of SDR and Gaussian randomization for solving (14). We validate that for 100 realizations and 1 interference 10^7 Gaussian randomizations are unable to yield to a feasible solution of (14). This motivates the techniques presented in Section IV.

B. Receive Beamforming Optimization Problem (Scenario B)

Let us consider the receive beamforming focuses on maximizing the received desired signal SINR [13]. For our case, the SINR can be written as

$$\text{SINR} = \frac{|\mathbf{u}^H \mathbf{H}\mathbf{t}|^2}{\sum_{m=1}^{M} P_{VSAT,m} |\mathbf{u}^H \mathbf{p}_m|^2 + \sigma_{FS}^2 \|\mathbf{u}\|^2}. \tag{20}$$

Bearing in mind that the SINR in (20) does not depend on the norm of the receive beamforming ($\|\mathbf{u}\|^2$), the receive beamforming that maximizes the SINR can be written as

$$\mathbf{u}^{\star} = \left(\sum_{m=1}^{M} P_{VSAT,m} \mathbf{p}_m \mathbf{p}_m^H + \sigma_{FS}^2 \mathbf{I} \right)^{-1} \widehat{\mathbf{h}}, \tag{21}$$

where

$$\widehat{\mathbf{h}} = \mathbf{H}\mathbf{t}. \tag{22}$$

In case we restrict the receive beamformer, $\mathbf{v}$ to be phase-only, we shall consider the following optimization problem

$$\begin{aligned} &\underset{\mathbf{u}}{\text{maximize}} \quad \frac{\mathbf{u}\widehat{\mathbf{H}}\mathbf{u}}{\mathbf{u}\mathbf{R}\mathbf{u}}, \\ &\text{subject to} \\ &|[\mathbf{u}]_n|^2 = 1/N_R \quad n = 1, \ldots, N_R, \end{aligned} \tag{23}$$

where

$$\mathbf{R} = \sum_{m=1}^{M} P_{VSAT,m} \mathbf{p}_m \mathbf{p}_m^H + \frac{\sigma_{FS}^2}{N_R} \mathbf{I}, \tag{24}$$

$$\widehat{\mathbf{H}} = \widehat{\mathbf{h}} \widehat{\mathbf{h}}^H. \tag{25}$$

The optimization problem in (23) is a difficult fractional quadratic optimization problem that does not admit a closed-form solution like for the digital case. In order to solve this problem, we consider the next change of variable

$$\mathbf{w} = \frac{\mathbf{u}}{\sqrt{\mathbf{u}^H \mathbf{R}\mathbf{u}}}, \quad \vartheta = \frac{1}{\mathbf{u}^H \mathbf{R}\mathbf{u}}. \tag{26}$$

With this, the optimization problem in (23), can be rewritten as

$$\begin{aligned} &\underset{\mathbf{w},\vartheta}{\text{maximize}} \quad \mathbf{w}^H \widehat{\mathbf{H}} \mathbf{w} \\ &\text{subject to} \\ &|[\mathbf{w}]_n|^2 = \vartheta/N_R \quad n = 1, \ldots, N_R, \\ &\mathbf{w}^H \mathbf{R}\mathbf{w} = 1. \end{aligned} \tag{27}$$

Note that once the optimization problem in (27) is solved, the optimal solution of the original problem is obtained such as

$$\mathbf{u}^{\star} = \mathbf{w}^{\star}/\vartheta^{\star}. \tag{28}$$

In any case, this last optimization problem presents the same difficulties as the transmit beamforming optimization due to phase-only constraints and the additional equality constraint $\mathbf{w}^H \mathbf{R}\mathbf{w} = 1$. Bearing this in mind, the next Section proposes to solve the problem of phase-only beamforming under spectrum sharing restrictions.

IV. Convex Relaxation Phase-Only Beamforming Techniques

This Section proposes two alternatives for efficiently phase-only beamforming optimization problems. Both approaches are novel solutions for the aforementioned problems and, as it is shown, they can provide approximate efficient solutions with a relatively low computational complexity.

A. SDP Concave-Convex Procedure

The optimization problem (17) can be written as

$$\underset{\mathbf{V} \succeq 0}{\text{maximize}} \quad \text{Tr}\left(\overline{\mathbf{H}}\mathbf{V}\right) \tag{29a}$$

$$\text{subject to} \tag{29b}$$

$$\text{Tr}\left(\mathbf{G}_k \mathbf{V}\right) \leq \epsilon_k \quad k = 1, \ldots, K, \tag{29c}$$

$$\text{Tr}\left(\mathbf{E}_n \mathbf{V}\right) = P/N_T \quad n = 1, \ldots, N_T, \tag{29d}$$

$$\text{Tr}\left(\mathbf{V}\right) - \lambda_{\max}\left(\mathbf{V}\right) \leq 0, \tag{29e}$$

where $\mathbf{E}_n$ is a matrix with zero entries instead the n-th diagonal element which is equal to one.

As discussed in [23], the constraint (29e) is equivalent to

$$\text{rank}\left(\mathbf{V}\right) = 1, \tag{30}$$

for any arbitrary semidefinite positive matrix $\mathbf{V}$. The optimization problem in (29) is non-convex due to the inequality in (29e) (i.e. $\lambda_{\max}\left(\mathbf{X}\right)$ is a convex function for $\mathbf{X}$ semidefinite positive). These type of non-convex problems can be solved via the concave-convex procedure, also known as sequential convex programming [30]. This method substitutes the non-convex (concave) parts of the problem by an affine approximation around an arbitrary point $\mathbf{Z}^{(k)}$. Given a feasible

initial point $\mathbf{Z}^{(0)}$, the method consists of sequentially solving the approximated optimization problem considering $\mathbf{Z}^{(k)}$ the previous optimal solution.

For our case, the affine approximation of $\lambda_{\max}(\mathbf{V})$ around matrix $\mathbf{Z}^{(k)}$ is given by [31]

$$\widehat{\lambda_{\max}}(\mathbf{V}) = \lambda_{\max}\left(\mathbf{Z}^{(k)}\right) + \mathrm{Tr}\left(\mathbf{z}_{\max}^{(k)}\mathbf{z}_{\max}^{(k),H}\left(\mathbf{V}-\mathbf{Z}^{(k)}\right)\right), \tag{31}$$

where $\mathbf{z}_{\max}^{(k)}$ is the eigenvector associated to the maximum eigenvalue of $\mathbf{Z}^{(k)}$. This approximation has considered that $\mathbf{z}_{\max}^{(k)}\mathbf{z}_{\max}^{(k),H}$ is a subgradient of $\lambda_{\max}\left(\mathbf{Z}^{(k)}\right)$ as reported in [31].

Since obtaining an initial feasible point $\mathbf{Z}^{(0)}$ is as challenging as obtaining a solution of (29), we resort to the penalty method. This mechanism replaces a set of constraints by adding a penalty function in the objective function. This penalty function shall be a measure of the replaced constraints violation. For our case, we elect and reformulate the approximate rank one constraint to act as a penalty function. With this, the optimization problem in (29) becomes

$$\begin{aligned}
&\underset{\mathbf{V}\succeq 0}{\text{maximize}} \quad \mathrm{Tr}\left(\overline{\mathbf{H}}\mathbf{V}\right) - \mu^{(k)}\mathrm{Tr}\left(\left(\mathbf{I}-\mathbf{z}_{\max}^{(k)}\mathbf{z}_{\max}^{(k),H}\right)\mathbf{V}\right) && \text{(32a)}\\
&\text{subject to} && \text{(32b)}\\
&\mathrm{Tr}\left(\mathbf{G}_k\mathbf{V}\right) \le \epsilon_k \quad k=1,\ldots,K, && \text{(32c)}\\
&\mathrm{Tr}\left(\mathbf{E}_n\mathbf{V}\right) = P/N_T \quad n=1,\ldots,N_T, && \text{(32d)}
\end{aligned}$$

where $\mu^{(k)}$ is a parameter that balances the penalty function importance over the whole objective function. For high values of $\mu^{(k)}$, the optimization focuses on obtaining a rank one solution whereas for low values of $\mu^{(k)}$, the optimization targets the maximization of the array gain towards the intended user.

By iterative solving (32) and updating $\mathbf{z}_{\max}^{(k)}$ with the eigenvector associated with the largest eigenvalue of the previous optimization solution, we can obtain an objective value solution of the optimization problem (17). As for general methods dealing with non-convex problems, the performance of the obtained solution depends on the proper election of $\mathbf{Z}^{(0)}$ and the value of $\mu^{(k)}$. In here, we consider an initial $\mathbf{Z}^{(0)}$ equal to the optimal problem of (29) without (29e). This initial point follows the heuristics that the optimal rank one solution shall be *close* to its high rank optimal design.

Furthermore, the parameter $\mu^{(k)}$ is initialized with a low value and increased at each iteration. With this, we ensure that at the first steps of the iteration, the algorithm is focused on the objective function optimization while for the latter steps, a rank one solution is obtained. The mechanism is depicted in Algorithm 1 where $\varkappa$ controls the convergence of the algorithm and κ guarantees the rank one of the final solution. Precisely, the value of κ shall be very low (10^{-3} at least) in order to obtain a rank one solution. We coin this scheme as SDP-CCP.

The algorithm presented in this Section suffers from certain drawbacks. First, the number of iterations can be high, leading to a very large computational complexity. In addition, at each iteration a SDP shall be solved whose worst-case asymptotic computational complexity is high. The next Section provides an alternative convex relaxation that yields to an efficient solution with a lower computational complexity scheme per iteration.

Data: $\mathbf{Z}^{(0)}$ from (29) without (29e) and $\mu^{(0)}$
Result: $\mathbf{v}^{\star}$
while $Tr(\mathbf{V}) - \lambda_{max}(\mathbf{V}) \le \kappa$ **do**
  Compute $\mathbf{V}^{(k)}$ according to (32).;
  if $\left\|\mathbf{V}^{(k)} - \mathbf{V}^{(k-1)}\right\| \le \varkappa$ **then**
    Update $\mu^{(k+1)} \leftarrow \left(\mu^{(k)}\right)^2$;
  else
    $k \leftarrow k+1$;
    $\mathbf{Z}^{(k+1)} \leftarrow \mathbf{V}^{(k)}$;
    Compute $\mathbf{z}_{\max}^{(k+1)}$;
  end
end
Output the final solution;

Algorithm 1: SDP-CCP procedure for phase-only spectrum sharing transmit beamforming techniques

Prior to presenting this alternative method, we describe the receive beamforming optimization. Given the optimization problem in (27), the SDP-CCP approach to this optimization problem can be written as

$$\begin{aligned}
&\underset{\mathbf{W}\succeq 0,\vartheta}{\text{maximize}} \quad \mathrm{Tr}\left(\widehat{\mathbf{H}}\mathbf{W}\right) - \mu^{(k)}\mathrm{Tr}\left(\left(\mathbf{I}-\mathbf{z}_{\max}^{(k)}\mathbf{z}_{\max}^{(k),H}\right)\mathbf{W}\right)\\
&\text{subject to}\\
&\mathrm{Tr}\left(\mathbf{E}_n\mathbf{W}\right) = \vartheta/N_R \quad n=1,\ldots,N_R,\\
&\mathrm{Tr}\left(\mathbf{R}\mathbf{W}\right) = 1.
\end{aligned} \tag{33}$$

For this case, we shall update at each iteration $\mathbf{Z}^{(k+1)} \leftarrow \mathbf{W}^{(k)}$ where $\mathbf{W}^{(k)}$ is the optimal solution in the k-th iteration. In this context, Algorithm 1 leads to an objective value solution of the problem in (27). Note that SDP-CCP always converge to a feasible solution as for high values of μ, the optimization problem yields to a rank one solution.

B. QCQP Penalty Convex-Concave Procedure

An alternative to the previous method is to consider the concave-convex procedure of the original optimization problem. By writing the optimization problem in (17) in standard form, we have

$$\begin{aligned}
&\underset{\mathbf{v}}{\text{minimize}} \quad -\mathbf{v}^H\overline{\mathbf{H}}\mathbf{v} && \text{(34a)}\\
&\text{subject to} && \text{(34b)}\\
&\mathbf{v}^H\mathbf{G}_k\mathbf{v} \le \epsilon_k \quad k=1,\ldots,K, && \text{(34c)}\\
&\mathbf{v}^H\mathbf{E}_n\mathbf{v} \le P/N_T \quad n=1,\ldots,N_T, && \text{(34d)}\\
&-\mathbf{v}^H\mathbf{E}_n\mathbf{v} \le -P/N_T \quad n=1,\ldots,N_T, && \text{(34e)}
\end{aligned}$$

Note that the set of equality constraints have been expanded in two sets of inequality constraints. By observing (34) it is indicated that the non-convexity of the problem is due to the objective function and the constraints in (34e). Now, in contrast to the previous case, we consider the penalized

convex-concave method *directly* to this optimization problem. This method approximates the concave parts of the problem by its first Taylor approximation and iteratively solves the equivalent problem. We describe this approximation for our case in the following.

For any $\mathbf{v}, \mathbf{z} \in \mathbb{C}^{N_T \times 1}$, the inequality

$$(\mathbf{v}-\mathbf{z})^H \mathbf{X} (\mathbf{v}-\mathbf{z}) \leq 0 \tag{35}$$

where $\mathbf{X} \in \mathbb{C}^{N_T \times N_T}$ is negative definite can be expanded by

$$\mathbf{v}^H \mathbf{X} \mathbf{v} \leq 2\mathcal{R}\left\{\mathbf{z}^H \mathbf{X} \mathbf{v}\right\} - \mathbf{z}^H \mathbf{X} \mathbf{z}. \tag{36}$$

Therefore, using the linear restriction around the point $\mathbf{z}$, we might replace the non-convex inequalities in (34) so that

$$\begin{aligned}
&\underset{\mathbf{v}}{\text{maximize}} \quad 2\mathcal{R}\left(\mathbf{z}^H \overline{\mathbf{H}} \mathbf{v}\right) - \mathbf{z}^H \overline{\mathbf{H}} \mathbf{z} \\
&\text{subject to} \\
&\mathbf{v}^H \mathbf{G}_k \mathbf{v} \leq \epsilon_k \quad k = 1, \ldots, K, \\
&\mathbf{v}^H \mathbf{E}_n \mathbf{v} \leq P/N_T \quad n = 1, \ldots, N_T, \\
&\mathbf{z}^H \mathbf{E}_i \mathbf{z} \leq -P/N_T + 2\mathcal{R}\left\{\mathbf{z}^H \mathbf{E}_i \mathbf{v}\right\} \quad n = 1, \ldots, N_T,
\end{aligned} \tag{37}$$

The optimization problem (37) is a second order cone programming (SOCP) that can be efficiently solved via interior point methods. Under this context, given an initial feasible value of $\mathbf{z}$, $\mathbf{z}^{(0)}$, iteratively solving (37) leads to a Karush-Kuhn-Tucker (KKT) point of (34) [32].

However, obtaining an initial feasible point $\mathbf{z}^{(0)}$ is as challenging as optimizing (34). In order to solve this problem, the authors in [20] impose the use of slack variables over all constraints and penalizing the objective function with its sum. Following this approach, the optimization problem at the n-th iteration can be described as

$$\begin{aligned}
&\underset{\mathbf{v}, \{s_m\}_{m=1}^{N_T}}{\text{maximize}} \quad 2\mathcal{R}\left\{\mathbf{z}^{H,(n)} \overline{\mathbf{H}} \mathbf{v}\right\} - \mathbf{z}^{H,(n)} \overline{\mathbf{H}} \mathbf{z}^{(n)} - \beta^{(n)} \sum_{m=1}^{N_T} s_m \\
&\text{subject to} \\
&\mathbf{v}^H \overline{\mathbf{G}_k} \mathbf{v} \leq \epsilon_k \quad k = 1, \ldots K, \\
&\mathbf{v}^H \mathbf{E}_i \mathbf{v} \leq P/N_T \quad i = 1, \ldots, N_T, \\
&\mathbf{z}^{H,(n)} \mathbf{E}_i \mathbf{z}^{(n)} \leq -P/N_T + 2\mathcal{R}\left\{\mathbf{z}^{H,(n)} \mathbf{E}_i \mathbf{v}\right\} + s_i \quad i = 1, \ldots, N_T, \\
&s_m \geq 0 \quad m = 1, \ldots, N_T,
\end{aligned} \tag{38}$$

where β is a regularization factor that controls the feasibility of the constraints. This regularization factor can be updated over the iterations. For our case, we consider a multiplicative update by a factor ρ. For high values of β, the optimization focuses on yielding to a feasible point of (29). For low values of β, the optimization problem targets to maximize the array gain towards the secondary user. The algorithm is summarized in Algorithm 2 and coined QCQP-PCCP.

As it can be observed, the proposed algorithm includes the stopping criteria $\left|\sum_{m=1}^{N_T} s_m\right| \leq \psi$. This condition guarantees that all the constraints of the original problem (34) are fulfilled for a sufficiently low ψ. Note that, it is possible to allow different maximum violations of each constraint by weighting the different components of the penalty function $\sum_{m=1}^{N_T} \beta_m^{(n)} s_m$.

Data: $\mathbf{z}^{(0)}$ and $\mu^{(0)}$
Result: $\mathbf{p}^\star$
while $\left|\sum_{m=1}^{2N_T} s_m\right| \leq \psi$ *and* $\|\mathbf{p}^{(n)} - \mathbf{p}^{(n-1)}\| \leq \omega$ **do**
  if $t < T_{max}$ **then**
    Compute $\mathbf{p}^{(n)}$ according to (38).;
    $\mathbf{z}^{(n+1)} \leftarrow \mathbf{p}^{(n)}$;
    $\beta^{(n+1)} \leftarrow \max\left(\rho\beta^{(n)}, \beta_{\text{max}}\right)$;
    $t \leftarrow n+1$;
  else
    $t \leftarrow 0$;
    Initialize with a new random value $\mathbf{z}^{(0)}$;
    Set up $\beta^{(0)}$ again;
  end
end
Output the final solution;

Algorithm 2: QCQP-PCCP optimization for phase-only beamforming optimization.

The role of β is to balance the optimization of the array gain to the intended users and the minimization of the constraint violation (i.e. for very high β the optimization problem seeks a feasible point rather than optimizing the array gain). We vary the value of β over the different iterations. First, we set a relatively low value of $\beta^{(0)}$ and; posteriorly, we sequentially increase this value. In other words, the proposed scheme first focuses on maximizing the array gain to the secondary user and, later, it seeks for a feasible solution. To avoid β taking a very large value when the number of iterations becomes large, leading to numerical difficulties, we consider a maximum β value β_{max}.

Algorithm 2 is not a descent algorithm as [20] mentions. With the aim of fostering the convergence, a maximum number of iterations T_{max} is imposed and, in case it is reached, we start with a new random initial point.

For the sake of completeness, let us formulate the QCQP-PCCP scheme of the receive beamforming optimization method

$$\begin{aligned}
&\underset{\mathbf{w}, \vartheta, \{s_m\}_{m=1}^{N_T+1}}{\text{maximize}} \quad 2\mathcal{R}\left\{\mathbf{z}^{H,(n)} \widehat{\mathbf{H}} \mathbf{w}\right\} - \beta^{(n)} \sum_{m=1}^{N_T+1} s_m \\
&\text{subject to} \\
&\mathbf{w}^H \mathbf{E}_i \mathbf{w} \leq \vartheta \quad i = 1, \ldots, N_T, \\
&\mathbf{z}^{H,(n)} \mathbf{E}_i \mathbf{z} \leq \vartheta + 2\mathcal{R}\left\{\mathbf{z}^{H,(n)} \mathbf{E}_i \mathbf{w}\right\} + s_i \quad i = 1, \ldots, N_T \quad , \\
&\mathbf{w}^H \mathbf{R} \mathbf{w} \leq 1 \\
&\mathbf{z}^{H,(n)} \mathbf{R} \mathbf{z} \leq 1 + 2\mathcal{R}\left\{\mathbf{z}^{H,(n)} \mathbf{R} \mathbf{w}\right\} + s_{N_T+1}, \\
&s_m \geq 0 \quad m = 1, \ldots, N_T + 1.
\end{aligned} \tag{39}$$

With this and Algorithm 2, we can achieve an objective value solution of the original phase-only receive optimization problem.

C. Computational Complexity Analysis

This Section aims at studying the computational complexities of the presented algorithms. Note that both schemes depend on the average number iterations which is a problem-dependent parameter that cannot be analytically obtained. Under this context, we assume that a total number of $Q_{\text{SDP-CCP}}$ and $Q_{\text{QCQP-PCCP}}$ iterations are required for the SDP convex-concave procedure and the QCQP penalized convex-concave procedure. We first consider the computational complexity of the transmit beamforming case and, later, we identify the computational complexity for the receive beamforming optimization case.

The SDP convex-concave procedure solves a SDP at each iteration. This SDP finds an efficient matrix of $N_T \times N_T$ dimensions with $2N_T + K$ constraints. On the contrary, the QCQP penalized convex-concave procedure approach requires to find a vector of $2N_T$ dimensions with a total number of constraints of $K + 3N_T$.

As discussed in [33], it is generally more convenient to solve a SOCP rather than a SDP via interior point methods. Indeed, it is known that the upper bound of number of iterations needed to find an efficient solution of SOCP is $\mathcal{O}\left(\sqrt{\mathcal{A}}\right)$ where $\mathcal{A}$ is the number of constraints of the SOCP. On the contrary, the worst case number of iterations in a SDP is $\mathcal{O}\left(\sum_{w=1}^{\mathcal{B}} u_w\right)$, where $\mathcal{B}$ is the total number of constraints and u_w the dimensions of the w-th constraint of the SDP.

In addition, at each iteration an interior point method requires a worst-case number of operations for the SDP of $\mathcal{O}\left(\mathcal{C}\sum_{w=1}^{\mathcal{B}} u_w^2\right)$, where $\mathcal{C}$ are the dimensions of the SDP variable. For SOCP, the computational complexity per iteration is reduced to $\mathcal{O}\left(\mathcal{D}\sum_{w=1}^{\mathcal{A}} v_w\right)$, where $\mathcal{D}$ are the dimensions of the SOCP variable and v_w the dimensions of the w-th constraint. Considering the above results, the computational complexity for the SDP convex-concave procedure becomes

$$\mathcal{M}_{\text{SDP-CCP}} = \mathcal{O}\left(Q_{\text{SDP-CCP}} N_T^6 \left(2N_T + K\right)^2\right), \quad (40)$$

By the asymptotic composition rule of computational complexity, the resulting computational complexity becomes

$$\mathcal{M}_{\text{SDP-CCP}} = \mathcal{O}\left(Q_{\text{SDP-CCP}} N_T^8\right), \quad (41)$$

where it has been assumed that $N_T \gg K$. This is the number of antennas is much higher than the number of FSS which is consistent with the system we are considering.

Bearing in mind the results for the SOCP, the computational complexity for the QCQP penalized convex-concave procedure is

$$\mathcal{M}_{\text{QCQP-PCCP}} = \mathcal{O}\left(Q_{\text{QCQP-PCCP}} \sqrt{2(K + 2N_T)} N_T^2 \left(2N_t + K\right)\right). \quad (42)$$

Under this context, the computational complexity of the QCQP-PCCP method becomes

$$\mathcal{M}_{\text{QCQP-PCCP}} = \mathcal{O}\left(Q_{\text{QCQP-PCCP}} N_T^{3.5}\right), \quad (43)$$

where it is evident the substantial computational complexity reduction with respect to SDP-CCP method in terms of the N_T exponential factor. From the analytical perspective it is difficult to derive an upper bound of the number of iterations of both methods. This is completed in the following Section.

It is important to remark that for the receive beamforming optimization, the same asymptotic computational complexity results are obtained in both cases. This is due the fact that the same order of magnitude of constraints and number of variables are employed for both the receive and transmit beamforming optimization cases.

Parameter	Value
P	24 dBW
Receive Antenna Gain	44 dB
σ^2_{FS}	-121 dBW
Distance between FS and FSS	$[1000, 20000]$ meters
θ	$[-10, 10]$ degrees
ϕ	$[-60, 60]$ degrees
Channel model parameters	$C = 1, L = 3$ degrees

TABLE I. FS SCENARIO DEFINITION

Parameter	Value
Distance	$35.78 \cdot 10^6$ meters
Satellite EIRP ($P_{\text{satellite}}$)	60 dBW
G_{max}	40 dB
P_{VSAT}	58 dBW
σ^2_{VSAT}	-121 dBW
Satellite Elevation Angle	40 degrees

TABLE II. FSS SCENARIO DEFINITION

V. NUMERICAL RESULTS

This Section presents the numerical evaluation of the proposed methods. To solve the described optimization problems we used CVX, a package for specifying and solving convex programs [34], [35]. This solver runs in a Windows desktop with 4 Intel i5 cores and 4GB of RAM. We consider 1000 Montecarlo runs for every numerical result.

As described in the previous sections, we consider the presence of FS and FSS in the same spectrum. We first describe the communication parameters of the FSS transmission in Table I. The distance between two FS and other FSS is assumed to be uniform random distributed between 1 and 20 Kms. Considering this distance, the elevation angle variation is low and assumed to be uniformly distributed between -10 and 10 degrees. In addition, ϕ is considered to be uniformly distributed between -60 and 60 degrees. As a backhaul scenario with long distances is assumed, we consider the channel model parameters of one cluster ($C = 1$) and $L = 3$ sub-rays.

The FSS communication link parameters are described in Table II. We consider a geostationary orbit (i.e. the satellite user terminal points to a fixed satellite) with an standard carrier-over-noise (C/N0) value of 10.5 dB. In addition, it is assumed that the satellite user terminal has an elevation angle of 40 degrees, a common value for Western countries. In all simulations we utilize the channel model described in Section II with the AoD, AoA, C and L described in Table I. We first evaluate the transmit beamforming method and then we describe the results for the receive beamforming case.

For both optimization frameworks, we assume

$$\mu^{(0)} = \beta^{(0)} = 10, \quad \chi = \psi = \omega = \kappa = \varkappa = 10^{-4}. \quad (44)$$

Moreover, for the QCQP-PCCP, we consider the following parameters

$$\beta_{\max} = 10^5, \quad T_{\max} = 30, \quad \rho = 10. \tag{45}$$

A. Transmit Beamforming (Scenario A)

Let us first consider the transmit beamforming case. Both proposed techniques are first compared in Figures 4 and 5. For obtaining these results we considered the case of $K = 1$ and $N_T = 36, 49, 64, 81$ and 100 transmit antenna elements. In addition, $\epsilon = -40$ dB. In Figure 4 we plot the performance loss defined as

$$\text{Loss}_{\text{Tx}} = 10 \log_{10} \left(\frac{\|\mathbf{Hv}\|^2}{\text{Tr}\left(\overline{\mathbf{H}}\mathbf{V}^*\right)} \right), \tag{46}$$

where $\mathbf{V}^*$ is the SDR solution of (17). The figure of merit of Loss_{Tx} describes how close the relaxation technique approximates to the upper bound solution of $\mathbf{V}^*$. For the QCQP-PCCP method we consider two initialization methods: a Gaussian randomization considering the covariance matrix of $\mathbf{V}^*$ and $\mathbf{I}$. The idea of using an initial random point considering $\mathbf{V}^*$ relays on the heuristic that the rank one solution should be *close* to its high rank solution.

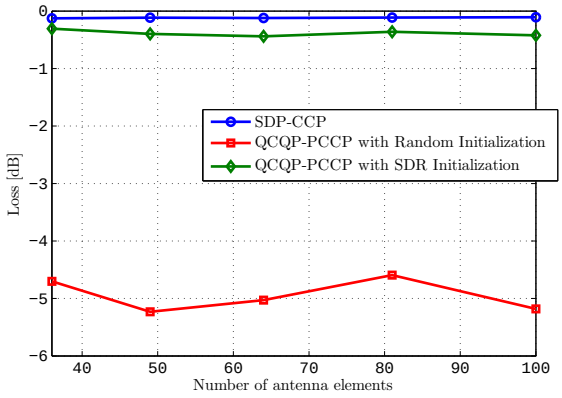

Fig. 4. Performance Loss for phase-only transmit beamforming optimization problem.

Considering the results in Figure 4, the method that behaves most closely to the upper bound is SDP-CCP. We observe a substantial difference between the two initialization alternatives: the QCQP-PCCP method using the SDR initialization shows a better performance compared to the case where the initial point is obtained pure randomly. In other words, the use of the SDR initialization is essential for obtaining an efficient solution with the QCQP-PCCP method.

The central processing unit time to compute a solution is described in Figure 5. It can be observed a large difference between SDP-CCP and QCQP-PCCP with both initializations. The performance gain of QCQP-PCCP is especially large when N_T increases. It is important to remark that the QCQP-PCCP presents a slightly better performance in CPU time when the SDR initialization is used.

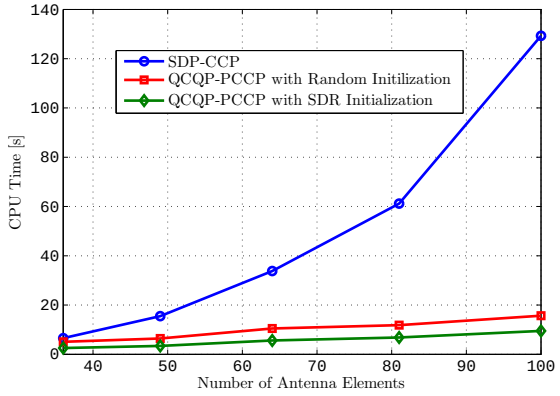

Fig. 5. Average CPU time versus number of antennas for phase-only transmit optimization problem.

Under this context, we can establish that QCQP-PCCP with SDR initialization is the method that presents the best CPU time and performance trade-off: its computational efficiency makes it appropriate to next generation multiantenna backhaul systems. Due to that, we use it for computing the achievable data rates in an scenario described by Table I. The results are depicted in Figure 6 where we plot the empirical cumulative distribution function of the average VSAT achievable rate defined as

$$R_{\text{VSAT}} = \frac{1}{K} \sum_{k=1}^{K} \frac{P_{\text{satellite}} G}{\sigma^2_{\text{VSAT}} + |\mathbf{g}_k^H \mathbf{v}|^2}. \tag{47}$$

We consider the case where K takes with equal probability the values of 1, 2 and 3 and $N_T = 49$. Furthermore, we include two cases $\epsilon = -30$ and $\epsilon = -50$ dBW.

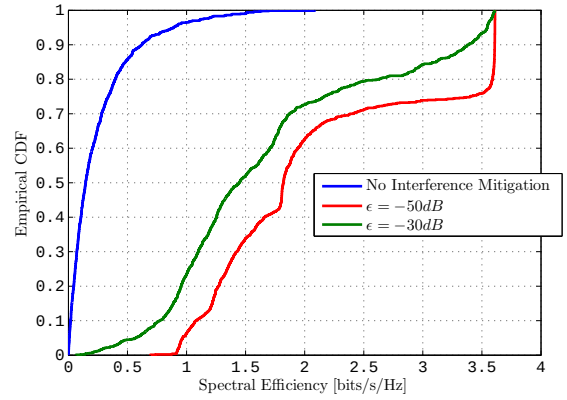

Fig. 6. Empirical cumulative distribution of the FSS achievable rates, R_{VSAT}, when optimizing the transmit beamforming with QCQP-PCCP with SDR initialization considering $N_T = 49$ and different ϵ values.

As it can be observed in Figure 6, the use of interference mitigation techniques is essential for providing a sufficiently large data rate for the satellite user terminals. Indeed, whenever

no interference mitigation techniques are used, it is observed that the data rates yield to very low values. As a matter of fact, the lower ϵ the larger the satellite achievable rates are obtained.

B. Receive Beamforming (Scenario B)

We now focus on the receive beamforming case. The losses figure of merit are computed such that

$$\text{Loss}_{\text{Rx}} = 10\log_{10}\left(\frac{|\widehat{\mathbf{h}}^H\mathbf{u}|^2\text{Tr}\left(\mathbf{R}\mathbf{U}^*\right)}{\text{Tr}\left(\widehat{\mathbf{H}}\mathbf{U}^*\right)\mathbf{u}^H\mathbf{R}\mathbf{u}}\right), \tag{48}$$

where $\mathbf{U}^*$ is the solution of the semidefinite relaxation of (23) and $\mathbf{u}$ is the obtained solution with the proposed optimization frameworks. As it can be observed in Figure 7, we observe a similar behaviour as in the transmit beamforming case: SDP-CCP is the one offering the lowest performance loss. In addition, the use of an SDR randomization as an initial point results in a better performance compared to the pure random initialization for the QCQP-PCCP as it happens with the transmit beamforming optimization.

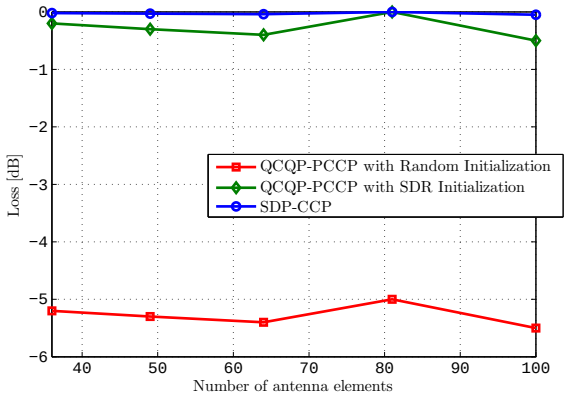

Fig. 7. Performance Loss for phase-only receive beamforming optimization problem.

On the other hand, the CPU time conducts differently to the transmit beamforming case. Considering the results in Figure 8, SDP-CCP is the solution offering the lowest average CPU time. Indeed, despite SDP-CCP obtains the highest worst case asymptotic computational complexity, the overall CPU time is lower compared to QCQP-PCCP with the two initialization alternatives. This is due to the average number of iterations required for each method. We observe that for the SDP-CCP most of the cases it is only required 2 or 3 iterations while for the QCQP-PCCP a number higher of 10 iterations is required.

In light of the above results, SDP-CCP scheme is the most adequate alternative for optimizing the receive beamforming case. This alternative is employed for obtaining the results in Figure 9 where we plot

$$R_{\text{FS}} = \log_2\left(1+\text{SINR}\right), \tag{49}$$

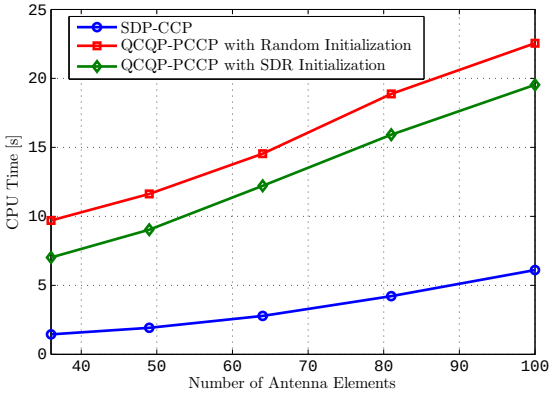

Fig. 8. Average CPU time versus number of antennas for phase-only receive optimization problem.

where SINR is defined in (20). As a benchmark, we consider the case where there is no interference (i.e. $P_{VSAT} = 0$). As it can be observed in Figure 9, despite the presence of interference, the receive beamforming design is able to offer an achievable rate similar to the case where no interference is present.

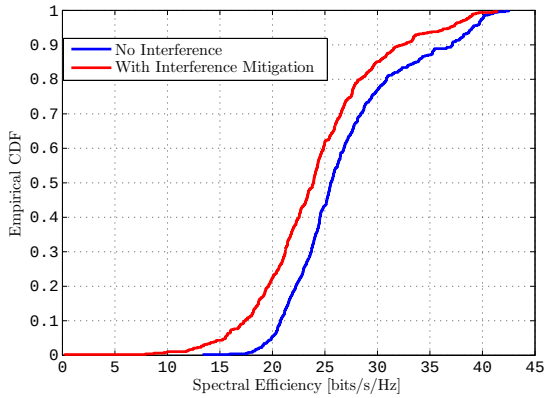

Fig. 9. Empirical cumulative distribution of the FS achievable rates, R_{FS}, when the FS receiver is equipped with $N_R = 49$ antennas and the optimization method used is SDP-CCP.

VI. Conclusions

This paper proposes the use of phased arrays in spectrum sharing satellite-terrestrial backhaul systems. In the considered scenario, interference between FS and FSS occurs and, in order to mitigate it, we propose two optimization frameworks for obtaining efficient transmit and receive beamforming designs. As discussed in the numerical evaluation, while for transmit beamforming QCQP-PCCP presents the best performance CPU time trade-off, for the receive beamforming case, SDP-CCP is the most convenient alternative as it shows a very low CPU time yet a very large performance gain. In both cases, the obtained array gain presents less than 1 dB loss

compared to the SDP upper bound. Considering the resulting spectral efficiencies and the reduced hardware implementation cost, the conceived techniques are promising solutions for next generation wireless spectrum sharing deployments in mmWave bands.

The beamforming techniques presented in this paper are key enabling components for both allowing an extraordinary increase of the spectrum usage for satellite systems and a potential spectrum license reduction for cellular operators. In other words, while currently there is no satellite deployments in the Ka shared band and no backhaul links in the exclusive satellite band, the use of the proposed multiantenna optimization techniques will enable those new spectrum applications.

REFERENCES

[1] J. P. Trufero and et al, "D2.1 - Review of Regulatory environment," SANSA Project (H2020-645047), Public Deliverable, Jan. 2016.

[2] F. Boccardi, H. Shokri-Ghadikolaei, G. Fodor, E. Erkip, C. Fischione, M. Kountouris, P. Popovski, and M. Zorzi, "Spectrum Pooling in MmWave Networks: Opportunities, Challenges, and Enablers," *IEEE Communications Magazine*, vol. 54, no. 11, pp. 33–39, November 2016.

[3] H. Shokri-Ghadikolaei, F. Boccardi, C. Fischione, G. Fodor, and M. Zorzi, "Spectrum Sharing in mmWave Cellular Networks via Cell Association, Coordination, and Beamforming," *IEEE Journal on Selected Areas in Communications*, vol. 34, no. 11, pp. 2902–2917, Nov 2016.

[4] A. K. Gupta, A. Alkhateeb, J. G. Andrews, and R. W. Heath, "Gains of Restricted Secondary Licensing in Millimeter Wave Cellular Systems," *IEEE Journal on Selected Areas in Communications*, vol. 34, no. 11, pp. 2935–2950, Nov 2016.

[5] A. K. Gupta, J. G. Andrews, and R. W. Heath, "On the Feasibility of Sharing Spectrum Licenses in mmWave Cellular Systems," *IEEE Transactions on Communications*, vol. 64, no. 9, pp. 3981–3995, Sept 2016.

[6] F. Guidolin, M. Nekovee, L. Badia, and M. Zorzi, "A study on the coexistence of fixed satellite service and cellular networks in a mmWave scenario," in *2015 IEEE International Conference on Communications (ICC)*, June 2015, pp. 2444–2449.

[7] ——, "A cooperative scheduling algorithm for the coexistence of fixed satellite services and 5G cellular network," in *2015 IEEE International Conference on Communications (ICC)*, June 2015, pp. 1322–1327.

[8] S. Maleki, S. Chatzinotas, B. Evans, K. Liolis, J. Grotz, A. Vanelli-Coralli, and N. Chuberre, "Cognitive spectrum utilization in Ka band multibeam satellite communications," *IEEE Communications Magazine*, vol. 53, no. 3, pp. 24–29, March 2015.

[9] E. Lagunas, S. K. Sharma, S. Maleki, S. Chatzinotas, and B. Ottersten, "Resource Allocation for Cognitive Satellite Communications With Incumbent Terrestrial Networks," *IEEE Transactions on Cognitive Communications and Networking*, vol. 1, no. 3, pp. 305–317, Sept 2015.

[10] P. Thompson and B. Evans, "Analysis of interference between terrestrial and satellite systems in the band 17.7 to 19.7 GHz," in *Communication Workshop (ICCW), 2015 IEEE International Conference on*. IEEE, 2015, pp. 1669–1674.

[11] S. Kutty and D. Sen, "Beamforming for Millimeter Wave Communications: An Inclusive Survey," *IEEE Communications Surveys Tutorials*, vol. 18, no. 2, pp. 949–973, Secondquarter 2016.

[12] S. Sun, T. S. Rappaport, R. W. Heath, A. Nix, and S. Rangan, "MIMO for millimeter-wave wireless communications: beamforming, spatial multiplexing, or both?" *IEEE Communications Magazine*, vol. 52, no. 12, pp. 110–121, December 2014.

[13] J. Yang and A. Swindlehurst, "Maximum SINR beamforming for correlated sources," in *1995 International Conference on Acoustics, Speech, and Signal Processing*, vol. 3, May 1995, pp. 1916–1919 vol.3.

[14] R. Zhang and Y. C. Liang, "Exploiting Multi-Antennas for Opportunistic Spectrum Sharing in Cognitive Radio Networks," *IEEE Journal of Selected Topics in Signal Processing*, vol. 2, no. 1, pp. 88–102, Feb 2008.

[15] P. Raviteja, Y. Hong, and E. Viterbo, "Analog Beamforming With Low Resolution Phase Shifters," *IEEE Wireless Communications Letters*, vol. 6, no. 4, pp. 502–505, Aug 2017.

[16] Z. Xiao, T. He, P. Xia, and X. G. Xia, "Hierarchical Codebook Design for Beamforming Training in Millimeter-Wave Communication," *IEEE Transactions on Wireless Communications*, vol. 15, no. 5, pp. 3380–3392, May 2016.

[17] S. Noh, M. D. Zoltowski, and D. J. Love, "Multi-Resolution Codebook and Adaptive Beamforming Sequence Design for Millimeter Wave Beam Alignment," *IEEE Transactions on Wireless Communications*, vol. 16, no. 9, pp. 5689–5701, Sept 2017.

[18] M. A. Vazquez, L. Blanco, A. Perez-Neira, and M. A. Lagunas, "Phase-Only Transmit Beamforming for Spectrum Sharing Microwave Systems," in *WSA 2016; 20th International ITG Workshop on Smart Antennas*, March 2016, pp. 1–7.

[19] A. L. Yuille and A. Rangarajan, "The concave-convex procedure," *Neural computation*, vol. 15, no. 4, pp. 915–936, 2003.

[20] T. Lipp and S. Boyd, "Variations and extension of the convex–concave procedure," *Optimization and Engineering*, vol. 17, no. 2, pp. 263–287, 2016. [Online]. Available: http://dx.doi.org/10.1007/s11081-015-9294-x

[21] Z.-Q. Luo, W.-K. Ma, A.-C. So, Y. Ye, and S. Zhang, "Semidefinite Relaxation of Quadratic Optimization Problems," *Signal Processing Magazine, IEEE*, vol. 27, no. 3, pp. 20–34, May 2010.

[22] O. Mehanna, K. Huang, B. Gopalakrishnan, A. Konar, and N. Sidiropoulos, "Feasible Point Pursuit and Successive Approximation of Non-Convex QCQPs," *Signal Processing Letters, IEEE*, vol. 22, no. 7, pp. 804–808, July 2015.

[23] A. H. Phan, H. D. Tuan, H. H. Kha, and D. T. Ngo, "Nonsmooth Optimization for Efficient Beamforming in Cognitive Radio Multicast Transmission," *IEEE Transactions on Signal Processing*, vol. 60, no. 6, pp. 2941–2951, June 2012.

[24] M. R. Akdeniz, Y. Liu, M. K. Samimi, S. Sun, S. Rangan, T. S. Rappaport, and E. Erkip, "Millimeter Wave Channel Modeling and Cellular Capacity Evaluation," *IEEE Journal on Selected Areas in Communications*, vol. 32, no. 6, pp. 1164–1179, June 2014.

[25] A. Maltsev and et al, "D5.1 - Channel Modeling and Characterization," MiWEBA Project (FP7-ICT-608637), Public Deliverable, Jan. 2014.

[26] T. S. Rappaport, Y. Xing, G. R. MacCartney, A. F. Molisch, E. Mellios, and J. Zhang, "Overview of Millimeter Wave Communications for Fifth-Generation (5G) Wireless Networks; With a Focus on Propagation Models," *IEEE Transactions on Antennas and Propagation*, vol. 65, no. 12, pp. 6213–6230, Dec 2017.

[27] I.-R. S.465-6, "Reference radiation pattern for earth station antennas in the fixed-satellite service for use in coordination and interference assessment in the frequency range from 2 to 31 GHz," Series of ITU-R Recommendations, Jan. 2016.

[28] D. Christopoulos, S. Chatzinotas, and B. Ottersten, "Weighted Fair Multicast Multigroup Beamforming Under Per-antenna Power Constraints," *IEEE Transactions on Signal Processing*, vol. 62, no. 19, pp. 5132–5142, Oct 2014.

[29] E. Karipidis, N. D. Sidiropoulos, and Z. Q. Luo, "Quality of Service and Max-Min Fair Transmit Beamforming to Multiple Cochannel Multicast Groups," *IEEE Transactions on Signal Processing*, vol. 56, no. 3, pp. 1268–1279, March 2008.

[30] P. D. Tao and L. T. H. An, "A D.C. Optimization Algorithm for Solving the Trust-Region Subproblem," *SIAM Journal on Optimization*, vol. 8, no. 2, pp. 476–505, 1998. [Online]. Available: http://dx.doi.org/10.1137/S1052623494274313

[31] H. D. Tuan, P. Apkarian, S. Hosoe, and H. Tuy, "D.C. optimization approach to robust control: Feasibility problems," *International Journal*

of Control, vol. 73, no. 2, pp. 89–104, 2000. [Online]. Available: http://dx.doi.org/10.1080/002071700219803

[32] G. R. Lanckriet and B. K. Sriperumbudur, "On the Convergence of the Concave-Convex Procedure," in *Advances in Neural Information Processing Systems 22*, Y. Bengio, D. Schuurmans, J. D. Lafferty, C. K. I. Williams, and A. Culotta, Eds. Curran Associates, Inc., 2009, pp. 1759–1767. [Online]. Available: http://papers.nips.cc/paper/3646-on-the-convergence-of-the-concave-convex-procedure.pdf

[33] M. S. Lobo, L. Vandenberghe, S. Boyd, and H. Lebret, "Applications of second-order cone programming," *Linear Algebra and its Applications*, vol. 284, no. 13, pp. 193 – 228, 1998, international Linear Algebra Society (ILAS) Symposium on Fast Algorithms for Control, Signals and Image Processing. [Online]. Available: http://www.sciencedirect.com/science/article/pii/S0024379598100320

[34] M. Grant and S. Boyd, "Graph implementations for nonsmooth convex programs," in *Recent Advances in Learning and Control*, ser. Lecture Notes in Control and Information Sciences, V. Blondel, S. Boyd, and H. Kimura, Eds. Springer-Verlag Limited, 2008, pp. 95–110, http://stanford.edu/~boyd/graph_dcp.html.

[35] ——, "CVX: Matlab Software for Disciplined Convex Programming, version 2.1," http://cvxr.com/cvx, Mar. 2014.